

PHYSICOCHEMICAL PROPERTIES OF PREPARED ZnO/ POLYSTYRENE NANOCOMPOSITES: STRUCTURE, MECHANICAL AND OPTICAL

S. M. AHMED^{a,*}, A. A. A. DARWISH^{c,d}, E. A. EL-SABAGH^b,
N. A. MANSOUR^a, D. E. ABULYAZIED^{a,c}, E. S. ALI^a

^a*Petrochemical Department, Egyptian Petroleum Research Institute (EPRI), Nasr City, Cairo, Egypt.*

^b*Physical Department, Faculty of Science, Al-Azhar University, Cairo, Egypt.*

^c*Nanotechnology Research Laboratory, Department of Physics, Faculty of Science, University of Tabuk, Tabuk, Saudi Arabia*

^d*Department of Physics, Faculty of Education at Al-Mahweet, Sana'a University, Al-Mahweet, Yemen*

^e*Department of Physics, Faculty of Science, University of Tabuk, Tabuk, Saudi Arabia*

Nanocomposites of polystyrene nano sphere (PS) with different loading of nano zinc oxide (ZnO) were prepared by two different methods, blend and in situ method. The prepared films of the synthesized nanocomposites materials were characterized by energy dispersive investigation (EDX), X-ray diffraction (XRD) and the morphology of ZnO/PS nanocomposite were investigated by transmission electron microscope (TEM). Phase composition and microstructure analysis shows that ZnO nanoparticles content has an influence on the crystal structure and morphology of ZnO/PS nanocomposite. The effect of ZnO nanoparticles on linear optical properties was studied in the PS lattice. The obtained results indicate that, the refractive index has been increased while the energy gap decreased with increasing ZnO nanoparticles contents. The improving of mechanical properties of ZnO/PS nanocomposite is verified due to the addition of ZnO nanoparticles.

(Received November 28, 2019; Accepted February 18, 2020)

Keywords: Polystyrene nano sphere, ZnO nanoparticles, Optical properties, Mechanical properties

1. Introduction

A great deal of effort has been made in recent years on organic / inorganic composite materials with different compositions. The combination of organic and inorganic materials leads to composites being formed that inherit the properties of both organic and inorganic components. In addition, improvements are made at very low loads in many of the properties relative to micron fillers [1].

Polymer nanocomposites have several applications based on their optical, electrical and mechanical properties [2–6]. Major features of PS include durability, transparency, high refractive index, good electrical insulation properties, low water absorption and fast handling, important for many industrial applications [7,8]. PS has excellent optical properties like color, chirality and high refractive index (1.60) [9]. PS is used as the host matrix for its ideal properties to investigate the optical characteristics of its nanocomposites [10].

Zinc oxide (ZnO) among the many inorganic materials is one of the most attractive semiconductors. In general, the addition of ZnO filler in polymer matrices can alter the optical, electrical and mechanical properties of polymers [11–15]. ZnO/PS nanocomposites can be used as anti-reflective coatings, as UV protective sheets and films, and as materials with increased thermal stability. The UV shielding applications for ZnO/PS nanocomposite films are reported [16].

*Corresponding author: daliaelsawy@hotmail.com

The optical study provides important information on the absorption, transmission and reflection of polymer films observed. The optical absorption and especially the absorption edge are a useful method to investigate the optically induced transition and to obtain information about the band structure, the band tail and the energy gap of the polymeric materials being considered [17, 18].

In the present study, two methods were used to prepare ZnO / PS nanocomposite samples, blend and in-situ method. In this work, the optical parameters will be discussed. The X-ray diffraction (XRD) and transmission electron microscopy (TEM) were used to investigate the dispersion of ZnO in PS matrix. The effect of contents and dispersion of ZnO on mechanical properties were studied.

2. Experimental

2.1. Materials

The chemicals used in this study were acquired from Aldrich Chemical Co.

Sodium dodecyl sulfate (analytical reagent, AR, 99.5%), potassium persulfate (AR, 99.5%), styrene (chemically pure, 99.0%), Zn (NO₃)₂, acetone and xylene.

2.2. Preparation of Polystyrene nanosphere

PS was prepared using polymerization with emulsion[19]. In a 250 ml two-neck flask, 0.15 g sodium dodecyl sulfate (SDS) and 0.1 g potassium persulfate were dissolved in 70 ml aqueous ethanol. Then, under the atmosphere of nitrogen (4.5 ml, 0.04 mol.) of styrene was added to the flask. To ensure polymerization, the resulting mixture was quickly stirred at 70°C for 8 h. The suspension was separated from the atmosphere of nitrogen and the material was washed and dried by de-emulsification. With Mwt about 65,000, the yield of prepared PS was about 70-75 percent.

2.3. Preparation of nano zinc oxide

100 mL of 0.05 M surfactant solution (SDS) was divided into two parts in the standard process. These two parts were used separately for the preparation of 0.5 M [Zn (NO₃)₂] metal precursors and 2 M NaOH. Using a dropping funnel under stirring, the NaOH solution was added. After NaOH was applied, the stirring was continued for 2 h. The precipitate was washed away with water and acetone. The product was dried in an electric oven at 110 °C. The dried product was then crushed and calcinated for 3 hours at 200 °C [20].

2.4. Preparation of ZnO/PS nanocomposites (Blend method)

The preparation of ZnO/PS nanocomposites by the blend method is based on the dispersion of nanometal oxides into the organic solvent by ultrasonic radiation for 10 min. Then the Nano zinc oxide colloid was combined in an appropriate ratio with PS dissolved in the same solvent in different weight % (0.0, 0.25, 0.5, 0.75 and 1). For maximum dispersion, the solution was dispersed by ultrasonic radiation for 20 min. and finally, after evaporation of the solvent, a transparent ZnO/PS nanocomposite film was obtained[21].

2.5. Preparation of ZnO/PS nanocomposites (In-situ method)

The preparation of ZnO/PS nanocomposites by the in-situ method is based on the addition of ZnO in different weight % (0.0, 0.25, 0.5, 0.75, and 1) during polystyrene prepared as the same method in 2.2.

2.6. Characterization and measurements

The specimen compositions were settled using the Energy Dispersive investigation of X-Ray beam (EDX) system, (Jeol sort JSM-T200, Japan). Micrographs for transmission electron microscopy (TEM) are taken using a micro-analyzer electron probe JEOL JX 1230 TEM. X-ray diffraction (XRD) measurements were performed at 40 kV generator voltage and 0.154 nm wavelength at room temperature on Philip's X-ray diffractometer PW1390 with CuK α Ni-filtered

radiation. At a speed of 2deg / min, the diffraction angle was scanned. The physicochemical properties of the prepared nanocomposites (the tensile strength, break elongation and Young's modulus) were determined using standard methods using an electronic Zwick tensile testing machine, model 1425. The measurements of transmittance, T and reflectance, R , spectra in the wavelength range (190-2500 nm) were carried out using V-670 UV-VIS-NIR double beam spectrophotometer. The optical T and R spectra were analyzed to determine the optical constants (such as absorption coefficient α , refractive index n) at every wavelength were calculated from the rectification values of T and R utilizing a private PC program [22]

3. Results and discussion

3.1. Structural characterizations:

The morphology of PS and ZnO nano particles is shown in Fig. 1 (a&b) and ZnO/PS nanocomposites is shown in Fig.2 (a &b). The image (Fig. 1a) of prepared PS spheres in SDS shows that the individual particles have smooth and bare surfaces. The PS spheres show good mono-disparity with diameters of 60-80 nm. While, the image of the prepared ZnO (**Fig. 1b**) indicated that the nanoparticles were highly crystalline, and could be well indexed to the hexagonal structure of pure metal oxides ZnO with average particle sizes of 11-28nm. Solans *et al.* [23] reported that self-assembled structures of various types can be formed in the binary system (water/surfactant), ranging, for example, from spherical and cylindrical micelles to lamellar phases, which can coexist with predominantly aqueous phases. So, the micelles route can be used to obtain the controlled shape and size of the Zinc oxide NPs. The metal precursors will interact in the solution with the surfactant molecules of SDS and there will be some chemical reactions and capping results.

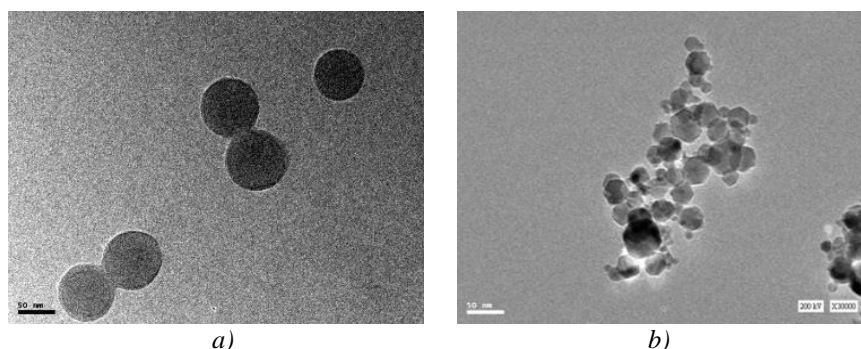


Fig. 1. TEM images of (a) PS nanosphere (b) nano ZnO.

In addition, the TEM image of ZnO/PS nanocomposites by blend method Fig.2a, The dark background was a polymer matrix with black dots showing ZnO nanoparticles distributed as a filler in the PS. Obviously, different charging capabilities of the filler and the polymer matrix led to the contrast between the nanoparticles and the polymer matrix. Fig.2b shows the TEM image of ZnO/PS nanocomposites by the in-situ method, it can be found that a well-defined core-shell structure with ZnO particles as core and PS as the shell has been formed. In the case of ZnO / PS nanocomposite in situ emulsion polymerization, the hydrophilic surfactant terminal (SDS) points to the water phase to ensure the stable suspension of the ZnO nanoparticles in the aqueous polymerization process. Due to the much larger surface area of the nano ZnO particles and the simpler adsorption of the monomer on the particle surface, the reaction site is preferred. The dispersed particles, which are regular in shape, have a distinct layer of PS chains grafted onto the surface of the zinc cores. The Fig.2b also displays ZnO cores with the diameter about 28 nm and the PS shell with the thickness about 72 nm. The EDX analysis ZnO/PS nanocomposite is shown in Fig.3, which shows the presence of Zn beside the presence of O₂.

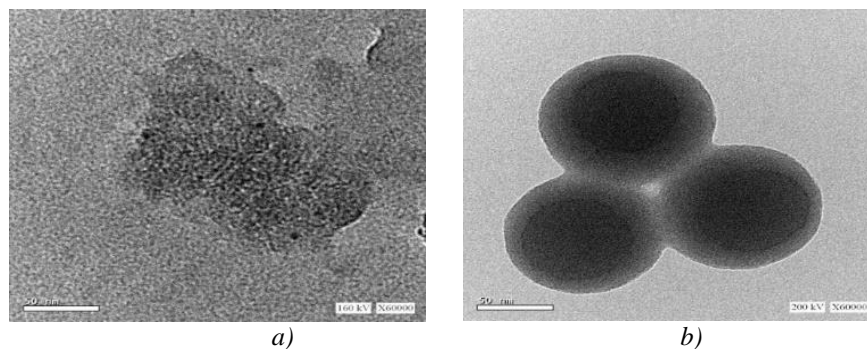


Fig. 2. TEM of ZnO/PS nanocomposites (a) blend method , (b) in-situ method.

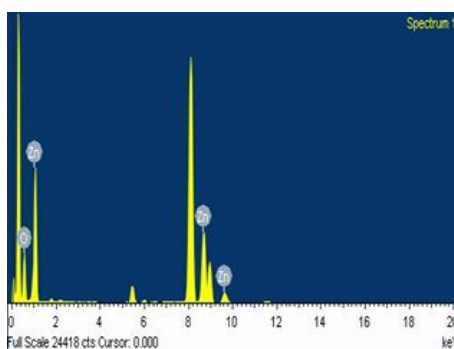


Fig. 3. EDX pattern of ZnO/PS nanocomposite particles.

X-ray diffraction spectra of pure nano PS and ZnO/ PS nanocomposites are shown in Fig.4. The XRD pattern of pure PS is specified by a broad diffraction peak at $2\theta=20^\circ$ indicated that the PS nanoparticles were amorphous materials. Fig.4 shows sharp diffraction peaks of ZnO can be observed at scattering angles (2θ) value of 31.83° , 34.49° , 36.26° , 47.59° , 56.56° , 62.86° , 68.12° , and 69.14° correspond to d spacing 2.81, 2.60, 2.47, 1.91, 1.62, 1.47, 1.37 and 1.35\AA , respectively[24], indicating that ZnO-filled PS nanocomposites consist of two phase structures, i.e. polymer and ZnO nanoparticles.

Meanwhile, XRD pattern of ZnO/PS nanocomposites prepared by in-situ Fig.5 shows a broad peak for PS and there is no diffraction peak originating from the ZnO in the XRD spectrum although with the ZnO content increasing, probably due to the ZnO is encapsulated in a polystyrene matrix. In the emulsion polymerization, the polystyrene adsorbed on the surface of ZnO to form a stable latex, which confirmed by TEM. Also, EDX (Fig.3) shows the characteristic peaks of both Zn and O_2 . It is clear that ZnO/PS nanocomposites were successfully synthesized.

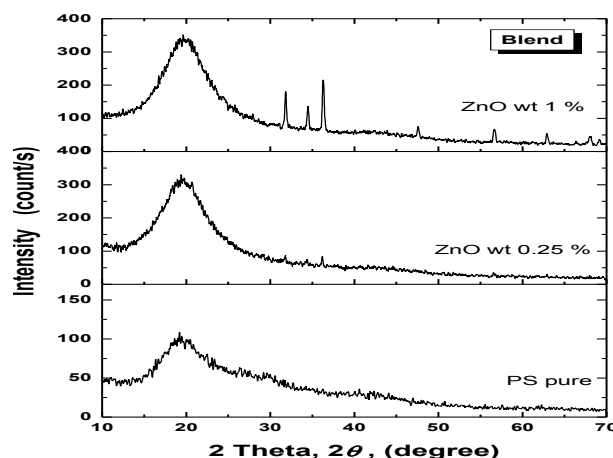


Fig. 4. XRD pattern of PS nanosphere. XRD pattern of ZnO/PS nanocomposite particles (blend) where (a) 0.25% and (b) 1% wt. of nanometals.

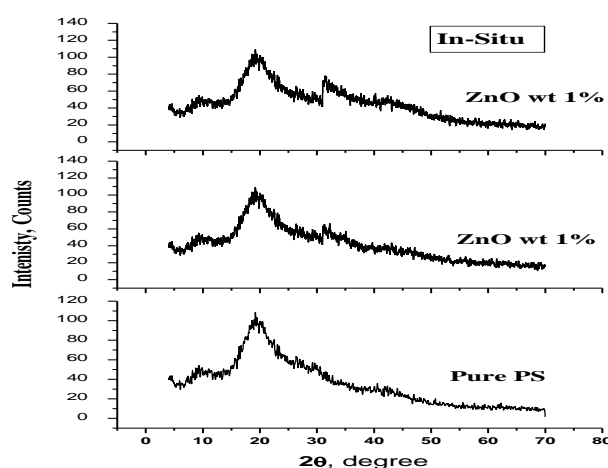


Fig. 5. XRD pattern of PS/ZnO composite particles (in-situ) where (a) 0.25% and (b) 1% wt. of nanometals.

3.2. Optical properties

The spectral distribution of both T and R for the blend ZnO/PS nanocomposites films of different weight % (0.0, 0.25, 0.5, 0.75 and 1.0) is presented in Fig. 6. The transmittance diminishes while reflectance increases with expanding filler concentration. This behavior of all doped PS samples with the increase in ZnO concentration can be assigned to the increase of the crystalline structure within the polymeric samples. The same behavior was observed for in-situ ZnO/PS nanocomposites films of different weight % (0.0, 0.25, 0.5, 0.75 and 1.0). Fig. 7 shows the optical transmittance and spectra as a function of λ of in-situ ZnO/PS nanocomposites films.

The spectra of α of matter close to the fundamental edge are critical for the examination of the kind of optical-electronic transitions and the energy bandgap. The relation between α and photon energy, $h\nu$, for the blend and in-situ ZnO/PS nanocomposites films of various weight % (0, 0.25, 0.5, 0.75 and 1) are represented in Fig. 8 (a, b). The gradient of α is from high to low photon energy. This implies the probability of transition of electrons is little in light of the fact that the energy isn't adequate to move the electrons from the valence band to the conduction band ($h\nu < E_g$). It was seen that at high energy, the values of α are high and the forbidden energy gap is less which shows the enormous probability of electronic transitions. Additionally, unmistakably the expansion of ZnO NPs concentration moves the absorption edge towards the higher energy.

In numerous materials, it is regular to analyze α at the fundamental edge according to band-to-band transitions theory. In this theory, α adheres to a power law, which is given by [25].

$$(\alpha h\nu)^m = G (h\nu - E_g) \quad (1)$$

where G is a constant. What's more, this equation yields estimations of the optical energy gap (E_g). Here m is a parameter that can take estimations of 2, 1/2, 1/3 or 3/2 relying upon the nature of the band to band electronic transitions. The data have been fitted with equation 1 for various estimations of m . The best fit is acquired for $m = 2$. This conduct showed that the transitions are direct allowed transitions. Fig. 9 (a, b) demonstrate the reliance of $(\alpha h\nu)^2$ on $h\nu$ for the blend and in-situ ZnO/PS nanocomposites films of various weight % (0, 0.25 0.5, 0.75 and 1). The got estimations of E_g from these curves are recorded in Table 1. The variety of the determined estimations of E_g may mirror the job of ZnO NPs in changing the electronic structure of the PS matrix because of the presence of different polaronic and imperfection levels [26, 27].

Table 1. The Optical parameters of ZnO/PS nanocomposites films.

PS/nanocomposite	E_g (eV)		E_o (eV)		E_d (eV)		ϵ_∞	
	In-situ	Blend	In-situ	Blend	In-situ	Blend	In-situ	Blend
PS	3.3		4.65		2.33		1.33	
0.25% wt ZnO	3.2	3	3.04	3.49	0.73	1.69	1.24	1.43
0.50% wt ZnO	3.1	2.8	4.24	4.03	1.36	1.97	1.32	1.49
0.75% wt ZnO	2.9	2.7	3.97	3.96	2.13	1.90	1.53	1.52
1.00% wt ZnO	2.4	2.5	2.48	3.93	0.31	2.33	1.12	1.59

The spectral dependences of n for the blend and in-situ ZnO/PS nanocomposites films of different weight % (0, 0.25 0.5, 0.75 and 1) are illustrated in Fig. 10 (a, b). The values of n increment because of filler expansion, this conduct can be credited to the expansion of the packing density because of filler content. The data of the reliance of n in the straightforward area at low optical frequencies were analyzed according to the single-oscillator model proposed by Wemple and Didomenico [26]. They presented energy parameters (scattering energy, E_d , and single oscillator energy, E_o) to depict the scattering of n . The refractive index can be communicated in the following equation [26]:

$$(n^2 - 1) = \frac{E_d E_o}{E_o^2 - (h\nu)^2}, \quad (2)$$

Blotting $(n^2 - 1)^{-1}$ against $(h\nu)^2$ as shown in Fig. 11 (a, b) for the blend and in-situ ZnO/PS nanocomposites films of different weight % (0.0, 0.25 0.5, 0.75 and 1.0) enables one to decide the estimations of E_o and E_d by fitting a straight line. The determined estimations of the scattering parameters and the relating high-frequency dielectric consistent, $\epsilon_\infty (= n^2)$, are recorded in Table 1.

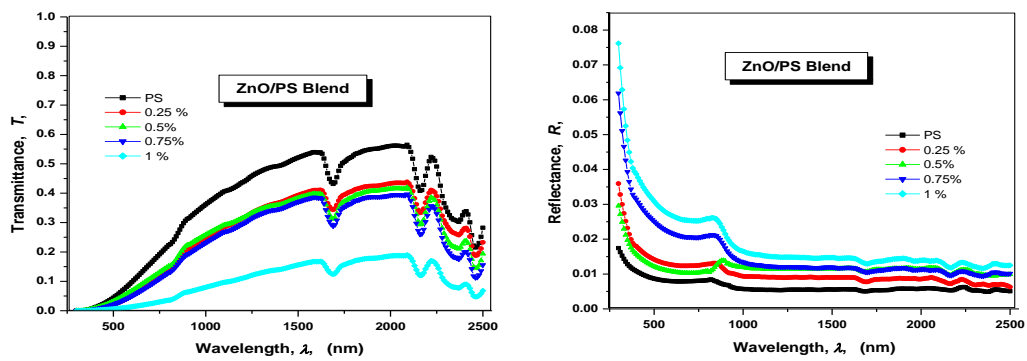


Fig. 6. Spectral distribution of normal incidence transmittance, T , and reflectance, R , for blend ZNO/PS nanocomposites films of different weight % (0, 0.25 0.5, 0.75 and 1).

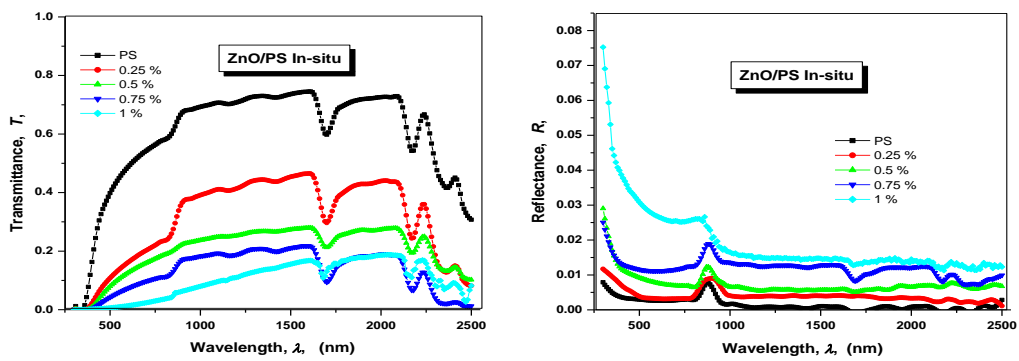


Fig. 7. Spectral distribution of normal incidence transmittance, T , and reflectance, R , for In-Situ ZnO/PS nanocomposites films of different weight % (0, 0.25 0.5, 0.75 and 1).

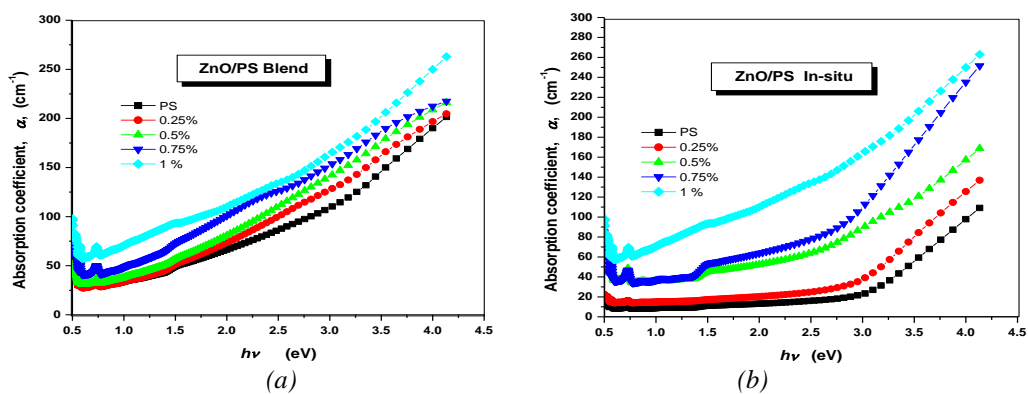


Fig. 8. Spectral behavior of absorption coefficient, α , for (a) blend and (b) in-Situ ZnO/PS nanocomposites films of different weight % (0, 0.25 0.5, 0.75 and 1).

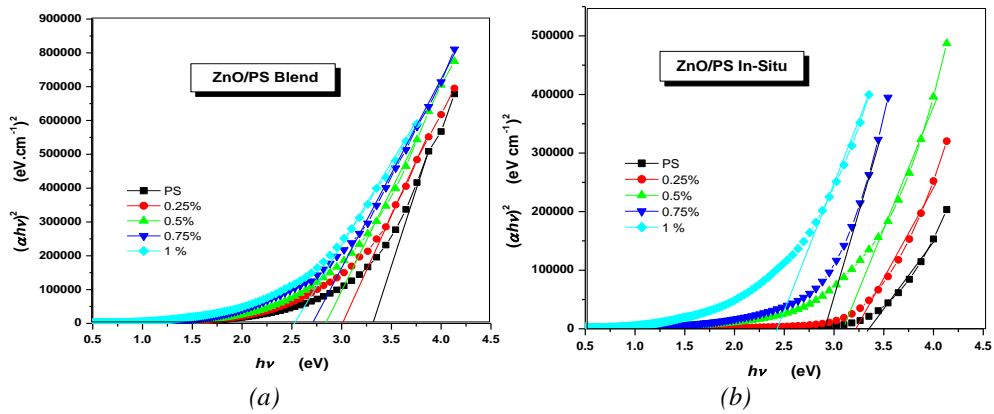


Fig. 9. Plot of $(\alpha h\nu)^2$ versus $h\nu$ (a) blend and (b) in-Situ ZnO/PS nanocomposites films of different weight % (0, 0.25 0.5, 0.75 and 1).

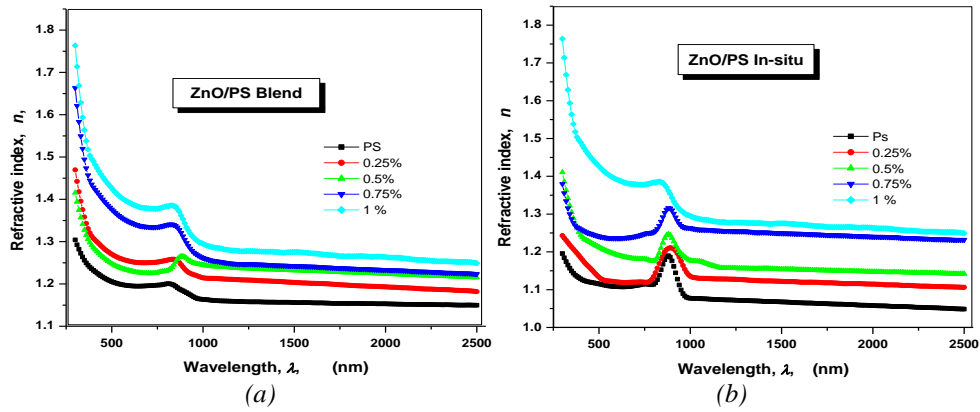


Fig. 10. Spectral behaviour of refractive index, n , for (a) blend and (b) in-situ ZnO/PS nanocomposites films of different weight % (0, 0.25 0.5, 0.75 and 1).

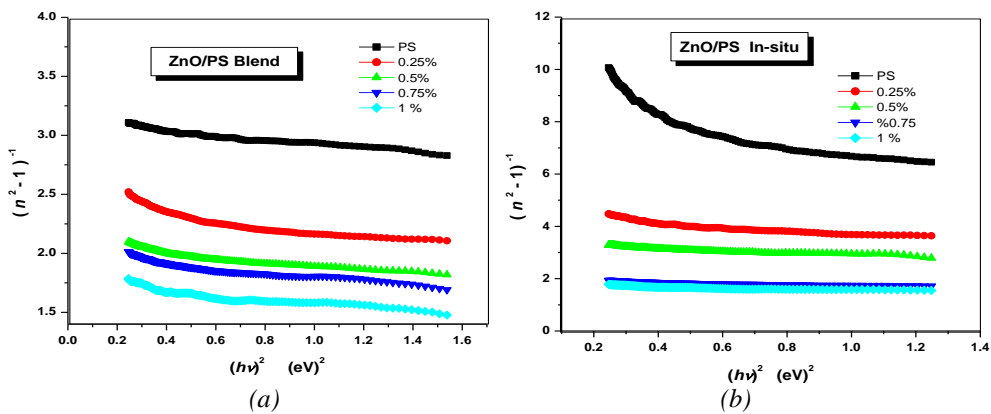


Fig. 11. Plots of $(n^2 - 1)^{-1}$ versus the photon energy $(h\nu)^2$ for (a) blend and (b) in-situ ZnO/PS nanocomposites films of different weight % (0, 0.25 0.5, 0.75 and 1).

3.4. Mechanical Properties

The mechanical properties of prepared nanocomposites are affected by many factors, the most important being the state of dispersion of the filler, the degree of crystallinity of the matrix and the filler-matrix interactions. The tensile strength, elongation at break and Young's modulus of ZnO/PS nanocomposites are shown in Fig. 12.

For the tensile strength, the figure reveals a notable increment for blend and in-situ samples with respect to neat PS. The general view of the figure shows also that the samples prepared by the in-situ method have higher values of tensile strength than that prepared by the blend method. It can be seen that the tensile strength of the blend samples has increased by 164% at 0.75 wt% nano ZnO than the pure PS, and then the tensile strength is nearly constant. While the tensile strength of the in-situ samples is has increased by also until 0.75 wt% nano ZnO than the pure PS, it reaches its maximum value at (210 % increase than pure PS). Interfacial interaction and adhesion between phases (which probably through bonds) may be the reason of the enhancement of tensile strength of the blend and in-situ samples than the pure PS. Increased tensile of the in-situ samples at the lower content of the nano ZnO particles could be a result of uniform dispersion of ZnO nanoparticles in the PS matrix. Particle agglomeration tends to reduce the strength of the blend samples than the in-situ samples in other words; agglomerates may act as strong stress concentrators [28].

Nevertheless, elongation at break gives an opposite behavior with the loading of ZnO nanoparticles in the PS matrix. The elongation for ZnO nanocomposites decreases for blend and in-situ methods than the pure PS. This reduction is attributed to stiffening of the matrix by the nano-particles which due to restrictions on the mobility of polymer chains during stretching by the tethering nano particles [29]. Chae, D.W et al [30] found that the introduction of ZnO nanoparticles into polystyrene (PS) decrease elongation at break. This implies that the interfacial adhesion is not strong enough to stand up to large mechanical forces.

Young's modulus as shown in figure gives the same behavior like tensile strength, increases with the content of ZnO nanoparticles for all the samples prepared by the two methods. It increased by 325 % for the blend samples, and 532 % for the in-situ samples at 0.75 wt% of the ZnO loadings respectively. Young's modulus is equivalent to the resistance to elastic deformation, thus the enhancement of modulus is reasonably attributed to the high resistance exerted by the rigid ZnO nanoparticles against the plastic deformation as well as the stretching resistance of the oriented backbone of polymer chains surrounded by ZnO.

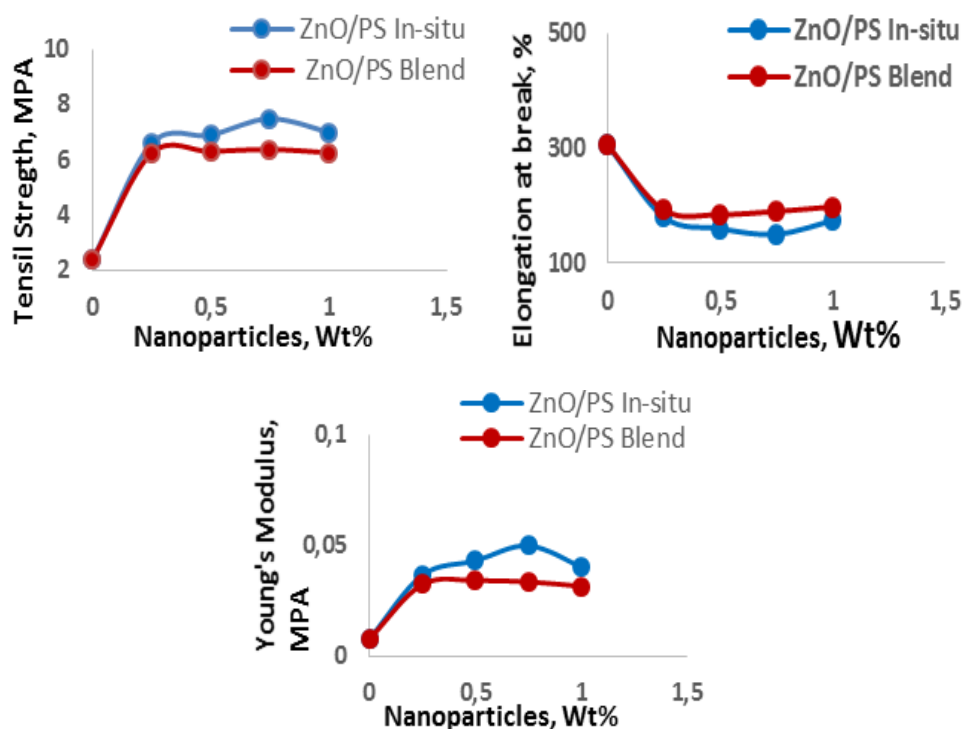


Fig. 12. The mechanical parameters for blend and in-situ ZnO/PS nanocomposites films as a function of ZnO weight %.

4. Conclusion

ZnO/PS nanocomposites were prepared by two different methods, blend and in-situ methods. The effect of the different concentrations of ZnO nanoparticles on the mechanical and optical properties of the nanocomposites were also taken into account.

Based on the results the following conclusions can be drawn:

Analysis of the phase composition and microstructure by TEM shows that the PS spheres show good mono-disparity with diameters of 60-80 nm. While, the image of the prepared ZnO indicated that the nanoparticles were highly crystalline. As well as, ZnO nanoparticles content has an influence on the crystal structure and morphology of ZnO/PS nanocomposite.

The effect of ZnO nanoparticles addition content in PS lattice on the linear optical properties has been studied. The obtained results indicate that, the refractive index has been increased while the energy gap decreased with increasing ZnO nanoparticles contents. The improving of mechanical properties is verified due to the addition of ZnO nanoparticles. Also ZnO/PS nanocomposite prepared by the in-situ method give enhanced mechanical properties than that prepared by the blend method. These results indicate the validity of the nanocomposites to be optic sensors.

References

- [1] M. Alexandre, P. Dubois, *Mater. Sci. Eng. R Reports* **28**, 1 (2000).
- [2] L. L. Beecroft, C. K. Ober, *Chem. Mater.* **9**, 1302 (1997).
- [3] R. Vijaya Kumar, R. Elgamiel, Y. Diamant, A. Gedanken, J. Norwig, *Langmuir* **17**, 1406 (2001).
- [4] E. M. Sadek, N. A. Mansour, S. I. Shara, A. M. Motawie, *J. Appl. Sci.* **7**, 535 (2011).
- [5] A. M. Motawie, M. M. Madany, A. Z. El-Dakrory, H. M. Osman, E. A. Ismail, M. M. Badr, D. A. El-Komy, D. E. Abulyazied, *Egypt. J. Pet.* **23**, 331 (2014).
- [6] O. O. Ayeleru, S. Dlova, F. Ntuli, W. K. Kupolati, P. A. Olubambi, *Procedia Manuf.* **30**, 194 (2019).
- [7] M. S. P. Shaffer and K. Koziol, *Chem. Commun.*, 2074 (2002).
- [8] J. P. Walker, S. A. Asher, *Anal. Chem.* **77**, 1596 (2005).
- [9] D. Sharma, P. Sharma, N. Thakur, *Optoelectron. Adv. Mater.* **3**, 145 (2009).
- [10] P. P. Jeeju, S. Jayalekshmi, K. Chandrasekharan, P. Sudheesh, *Opt. Commun.* **285**, 5433 (2012).
- [11] J. Lee, D. Bhattacharyya, A. J. Easteal, J. B. Metson, *Curr. Appl. Phys.* **8**, 42 (2008).
- [12] D. W. Chae, B. C. Kim, *Polym. Adv. Technol.* **16**, 846 (2005).
- [13] E. Tang, S. Dong, *Colloid Polym. Sci.* **287**, 1025 (2009).
- [14] J. Thapoung, K. Tasurin, N. Traiphol, N. Pangpaiboon, *J. Met. Mater. Miner.* **28**, 89 (2018).
- [15] M. Kiaei, B. Kord, A. Samariha, Y. R. Moghdam, M. Farsi, *BioResources* **12**, 6518 (2017).
- [16] W.-C. Shih, M.-S. Wu, *J. Cryst. Growth* **137**, 319 (1994).
- [17] S. H. Deshmukh, D. K. Burghate, S. N. Shilaskar, G. N. Chaudhari, P. T. Deshmukh, *Indian J. Pure Appl. Phys.* **46**, 344 (2008).
- [18] A. El-Khodary, *Phys. B Condens. Matter* **405**, 3401 (2010).
- [19] S. Tang, L. Chen, S. Vongehr, X. Meng, *Appl. Surf. Sci.* **256**, 2654 (2010).
- [20] S. M. Abdel-Azim, A. K. Aboul-Gheit, S. M. Ahmed, D. S. El-Desouki, M. S. A. Abdel-Mottaleb, *Int. J. Photoenergy* **2014**, 1 (2014).
- [21] M. Marinović-Cincović, Z. V. Šaponjić, V. Djoković, S. K. Milonjić, J. M. Nedeljković, *Polym. Degrad. Stab.* **91**, 313 (2006).
- [22] A. A. A. Darwish, H. A. M. Ali, *J. Alloys Compd.* **710**, 431 (2017).
- [23] C. Solans, P. Izquierdo, J. Nolla, N. Azemar, M. J. Garcia-Celma, *Curr. Opin. Colloid Interface Sci.* **10**, 102 (2005).
- [24] M. Kheirandish, S. Borhani, *World Acad. Sci. Eng. Technol. Int. J. Chem. Mol. Nucl. Mater. Metall. Eng.* **8**, 192 (2014).
- [25] M. M. El-Nahass, K. F. Abd-El-Rahman, A. A. M. Farag, A. A. A. Darwish, *Int. J. Mod.*

- Phys. B **18**, 421 (2004).
- [26] V. S. Sangawar, R. J. Dhokne, A. U. Ubale, P. S. Chikhalikar, S. D. Meshram, Bull. Mater. Sci. **30**, 163 (2007).
- [27] D. E. Abulyazied, E. F. M. E.- Zaidia, **14**, 359 (2018).
- [28] A. Alam, A. H. Ansari, 355 (2014).
- [29] I.-Y. Jeon, J.-B. Baek, Materials (Basel). **3**, 3654 (2010).
- [30] D. W. Chae, B. C. Kim, Polym. Adv. Technol. **16**, 846 (2005).